



Basic Quantitative Imaging Approaches

1

Daniel Thomas Ginat

1.1 Line and Angle Measurements

A typical picture archive and communication system (PACS) image viewer offers a basic palette of measurements, including the commonly used line and angle functions (Fig. 1.1), which can be drawn manually by the user on the images of interest.

Measurements are typically made using the metric system. It should be cautioned that systems that display line and angle measurements to one-tenth of a millimeter or degree do not actually have the accuracy to justify so many significant digits. Another pitfall regarding line measurements on cross-sectional imaging is that these can be affected by variations in the patient positioning (Fig. 1.2). This issue can be mitigated by implementing the standard positioning of patients in scanners or reformatting the images such that they are consistent between exams.

Most anatomic structures in the population have a normal distribution of size. Reference normative measurements available in the literature and in the subsequent chapters in this book are often

D. T. Ginat (✉)

Department of Radiology, Section of Neuroradiology,
University of Chicago, Chicago, IL, USA
e-mail: dtg1@uchicago.edu

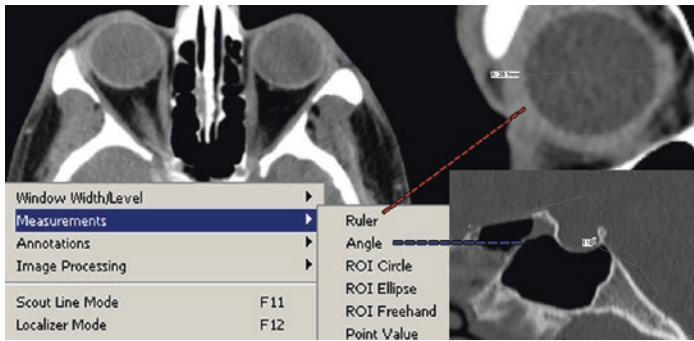


Fig. 1.1 Screenshot of the measurement palette on PACS with example ruler and angle markers

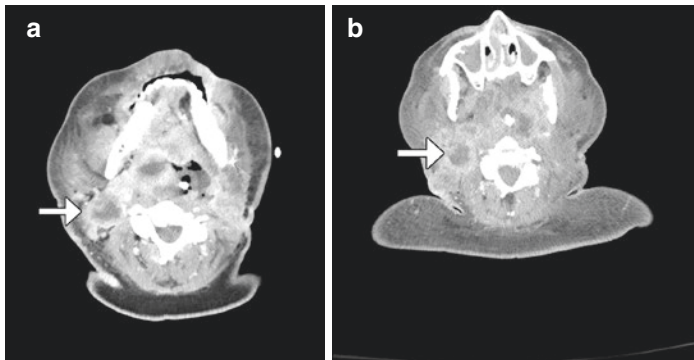


Fig. 1.2 Sequential computed tomography (CT) images (**a** and **b**) at the level of a necrotic right cervical lymph node (arrows) show differences in angulation of the patient, in which the lesion is at the level of the maxillary sinuses on one image and at the level of the teeth on the other image

reported as averages of sample populations, sometimes along with standard deviations, ranges, or 95% confidence intervals (CI), which quantify the degree of variation that measurements have within a sample population. These statistical parameters can be used as guidelines to help decide whether measurements obtained on particular scans are normal or abnormal.

1.2 Area and Volume Measurements

For many clinical applications, size is better represented in terms of cross-sectional areas and volumes than unidimensional measurements, especially for structures with an irregular shape. There are several techniques for determining volume on imaging, including the following:

- The prorated ellipsoid formulas for the cross-sectional area and volume:

$$\text{Area} = \pi \times \text{length} \times \text{width}$$

$$\text{Volume} = 0.52 \times \text{height} \times \text{length} \times \text{width}$$

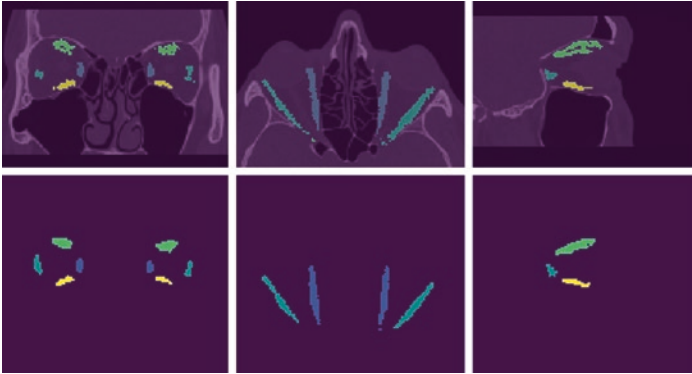
Although straightforward, these formulas can be less accurate if the shape deviates substantially from a circle or sphere.

- Planimetry is a more reliable, but more time-consuming, method for measuring volume in which the edge of the structure is traced on all image slices and cross-sectional areas are summed and multiplied by the slice thickness.
- Specialized software can be used to recognize the edges of structures, for example, using threshold-based, connected components, or region-growing algorithms, to segment an organ or lesion and thereby automate determination of volumes (Fig. 1.3).

In general, thin slice reconstructions of 1 mm or at least no more than 3 mm are recommended for reliable volume measurements on cross-sectional imaging.

1.3 CT Attenuation and MRI Signal Intensity Measurements

In addition to measuring the size of a structure, the value of the pixel intensity can be ascertained. This can be accomplished by drawing a region of interest on the image. On computed



Volume (mm³)
 Medial rectus, Lateral, Superior (+Superior Levator Palpabrae), Inferior rectus
 2177, 1888, 2453, 1660

Fig. 1.3 Volume measurements of the extraocular muscles generated using machine learning automatic segmentation. Courtesy of Ramkumar Rajabathar Babu Jai Shanker

tomography (CT), the region of interest can provide measurement of attenuation via Hounsfield units (HU). Different tissues and materials have characteristic attenuation values (Fig. 1.4). On magnetic resonance imaging (MRI), T1- and T2-weighted signal intensity can also be measured using regions of interest, as well as the diffusivity of protons on apparent diffusion coefficient (ADC) maps derived from diffusion-weighted imaging (Fig. 1.5).

1.4 Measurement Errors

There are three main types of measurement errors: systematic errors, random errors, and gross errors:

- Systematic errors lead to inaccurate measurements that trend in one direction and occur due to fault in the measuring device, including scanners. This can manifest with partial volume averaging, in which the computed tomography (CT) attenuation

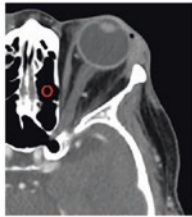
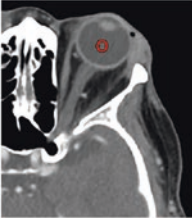

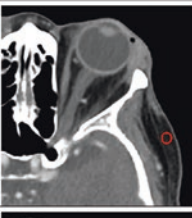

Tissue/Material	CT	Attenuation (HU)
Air		-1000
Fluid (CSF, vitreous)		0 to 15
Brain		20 to 45
Fat		-200 to -50
Bone		200 to 1000

Fig. 1.4 Schematic showing the typical attenuation values of different materials and tissues on computed tomography (CT)

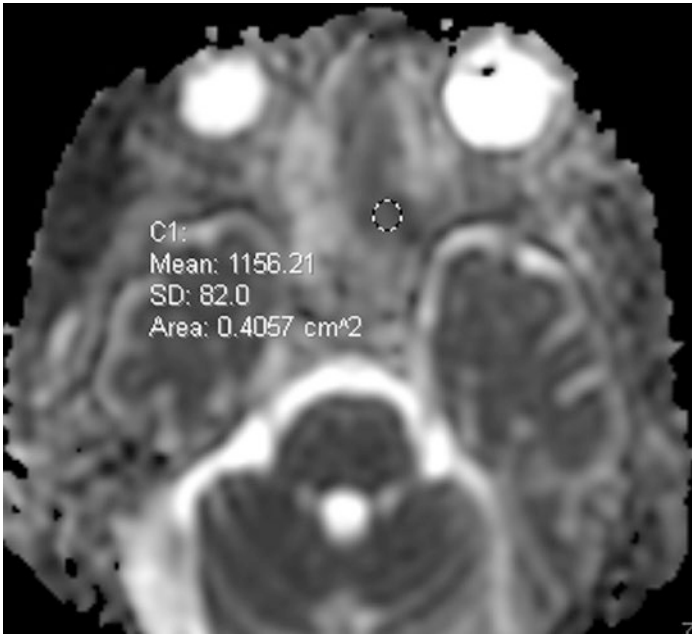


Fig. 1.5 ADC map shows a diffusion region of interest (ROI) positioned on a left sinonasal tumor

or MRI signal of a structure within a voxel blends with other structures. This is particularly noticeable between low versus high magnification images. At low magnification, the edges of certain structures can appear rather distinct, but at increasing degrees of magnification, the edge is actually blurry (Fig. 1.6). The width of this gray zone is particularly significant relative to structures of submillimeter size, which can render the measurement inaccurate. Such issues can be mitigated by using ultrathin-section acquisition.

- Random errors lead to inconsistent variations in measurement. This can be attributable to the inherent noise in images

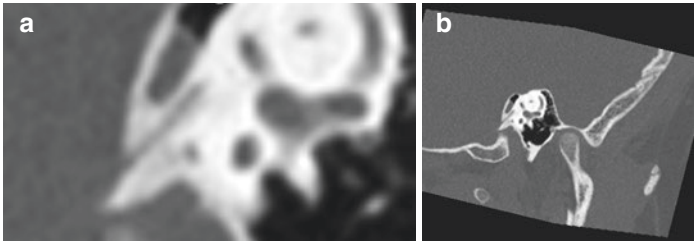


Fig. 1.6 Sagittal oblique computed tomography (CT) images without (a) and with (b) magnification show that the anatomical margins become blurred with magnification

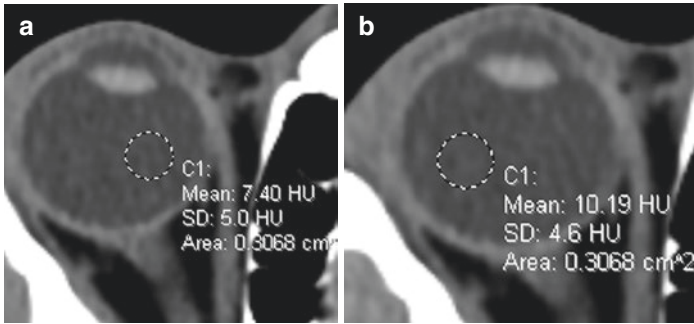


Fig. 1.7 Axial computed tomography (CT) images (a and b) show the different attenuation measurements of the globe contents at slightly different positions due to noise, each with substantial standard deviations

(Fig. 1.7) and factors such as intraobserver and interobserver variability, whereby the same individual will obtain different measurements of the same thing at different times or different individuals will obtain different measurements of the same thing.

- Gross errors are those in which the wrong measurement is recorded, such as entering 18 mm instead of 13 mm, for example.

Further Reading

- Abramson RG, Burton KR, Yu JP, Scalzetti EM, Yankeelov TE, Rosenkrantz AB, Mendiratta-Lala M, Bartholmai BJ, Ganeshan D, Lenchik L, Subramaniam RM. Methods and challenges in quantitative imaging biomarker development. *Acad Radiol.* 2015;22(1):25–32.
- Buerke B, Puesken M, Beyer F, et al. Semiautomatic lymph node segmentation in multislice computed tomography: impact of slice thickness on segmentation quality, measurement precision, and interobserver variability. *Invest Radiol.* 2010;45(2):82–8.
- Dejaco D, Url C, Schartinger VH, et al. Approximation of head and neck cancer volumes in contrast enhanced CT. *Cancer Imaging.* 2015;15:16. Published 2015 Sep 29.
- Fabel M, Wulff A, Heckel F, et al. Clinical lymph node staging—influence of slice thickness and reconstruction kernel on volumetry and RECIST measurements. *Eur J Radiol.* 2012;81(11):3124–30.
- Fehlings MG, Furlan JC, Massicotte EM, et al. Interobserver and intraobserver reliability of maximum canal compromise and spinal cord compression for evaluation of acute traumatic cervical spinal cord injury. *Spine (Phila Pa 1976).* 2006;31(15):1719–25.
- Ginat DT, Gupta R. Advances in computed tomography imaging technology. *Annu Rev Biomed Eng.* 2014;16:431–53.
- Juliano AF, Ting EY, Mingkwansook V, Hamberg LM, Curtin HD. Vestibular aqueduct measurements in the 45° oblique (Pöschl) plane. *AJNR Am J Neuroradiol.* 2016;37(7):1331–7.
- Mueller S, Wichmann G, Dornheim L, et al. Different approaches to volume assessment of lymph nodes in computer tomography scans of head and neck squamous cell carcinoma in comparison with a real gold standard. *ANZ J Surg.* 2012;82(10):737–41.
- Rosenkrantz AB, Mendiratta-Lala M, Bartholmai BJ, Ganeshan D, Abramson RG, Burton KR, Yu JP, Scalzetti EM, Yankeelov TE, Subramaniam RM, Lenchik L. Clinical utility of quantitative imaging. *Acad Radiol.* 2015;22(1):33–49.
- Wilson JD, Eardley W, Odak S, Jennings A. To what degree is digital imaging reliable? Validation of femoral neck shaft angle measurement in the era of picture archiving and communication systems. *Br J Radiol.* 2011;84(1000):375–9.
- Zhu W, Huang Y, Zeng L, et al. AnatomyNet: deep learning for fast and fully automated whole-volume segmentation of head and neck anatomy. *Med Phys.* 2019;46(2):576–89.